iScience

CellPress
OPEN ACCESS

Article

Indole-3-propionic acid regulates lateral root development by targeting auxin signaling in *Arabidopsis*

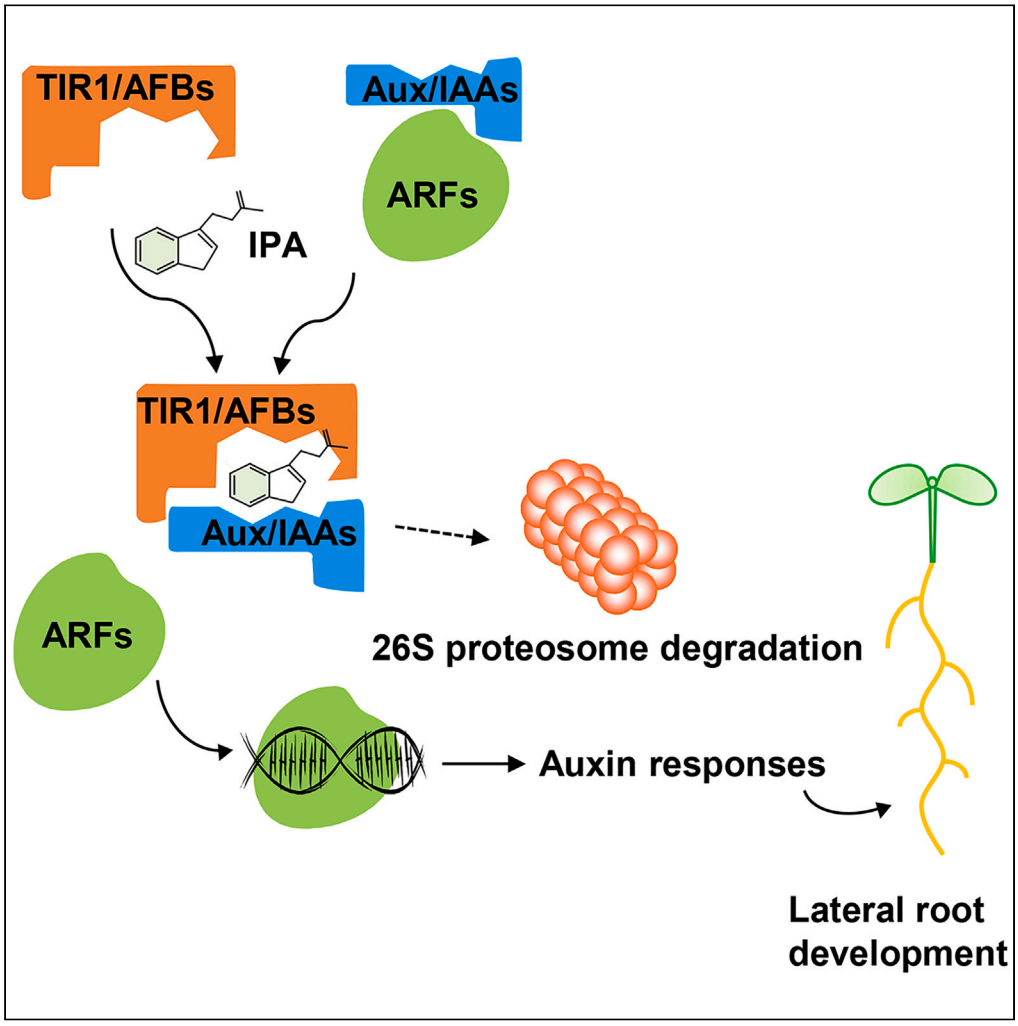

Yue Sun, Zhisen Yang, Caoli Zhang, ..., Xin Liu, Linfeng Sun, Shutang Tan

lx023@ustc.edu.cn (X.L.)
sunlf17@ustc.edu.cn (L.S.)
sttan@ustc.edu.cn (S.T.)

Highlights

IPA regulates *Arabidopsis* lateral root development

IPA modulates auxin responses in *Arabidopsis*

IPA functions through the TIR1/AFB-Aux/IAA auxin signaling pathway

IPA directly targets the TIR1/AFB-Aux/IAA complexes

Sun et al., iScience *27*, 110363
July 19, 2024
https://doi.org/10.1016/j.isci.2024.110363

iScience

CellPress
OPEN ACCESS

Article

Indole-3-propionic acid regulates lateral root development by targeting auxin signaling in *Arabidopsis*

Yue Sun,[1,2] Zhisen Yang,[1,2] Caoli Zhang,[1,2] Jing Xia,[1,2] Yawen Li,[1] Xin Liu,[1,*] Linfeng Sun,[1,*] and Shutang Tan[1,3,*]

SUMMARY

Indole-3-propionic acid (IPA) is known to be a microbe-derived compound with a similar structure to the phytohormone auxin (indole-3-acetic acid, IAA). Previous studies reported that IPA exhibited auxin-like bioactivities in plants. However, the underlying molecular mechanism is not totally understood. Here, we revealed that IPA modulated lateral root (LR) development via auxin signaling in the model plant *Arabidopsis thaliana*. Genetic analysis indicated that deficiency of the TIR1/AFB-Aux/IAA-ARF auxin signaling pathway abolished the effects of IPA on regulating LR development. Further biochemical, transcriptomic profiling and cell biological analyses revealed that IPA directly bound to the TIR1/AFB-Aux/IAA coreceptor complex and thus activated downstream gene expression. Therefore, our work revealed that IPA is a potential signaling molecule that modulates plant growth and development by targeting the TIR1/AFB-Aux/IAA-mediated auxin signaling pathway, providing potential insights into root growth regulation in plants.

INTRODUCTION

Auxin is an essential phytohormone involved in almost every aspect of plant growth and development.[1–3] Our current understanding of the molecular mechanisms underlying auxin biosynthesis, metabolism, transport, and signaling has advanced through decades of genetic studies.[3–5] The major natural form of auxin is indole-3-acetic acid (IAA), whose biosynthesis is mainly catalyzed by the TRYPTOPHAN AMINOTRANSFERASE OF ARABIDOPSIS (TAA1)/TRYPTOPHAN AMINOTRANSFERASE-RELATED PROTEIN (TAR) and YUCCA (YUC) enzymes in plants.[6,7] Additionally, microbes can synthesize IAA, which is a key link between plants and microbes in ecosystems. Microbe-derived IAA can promote the growth of infected plant tissues, subsequently benefiting their own growth.[8]

A key feature of auxin is its polar transport across cells, namely polar auxin transport (PAT), which is ensured by plasma membrane (PM)-localized PIN-FORMED (PIN) exporters[9–13] and AUXIN1 (AUX1)/LIKE AUXIN1 (LAX) importers.[14,15] Genetic data suggest that ATP-binding cassette subfamily B/multidrug resistance/phosphoglycoprotein (ABCB/MDR/PGP) ABCB1 and ABCB19 are also involved in PAT in *Arabidopsis*.[16–18] However, recent studies suggest that brassinosteroids but not auxins are the substrates of ABCB19.[19] Moreover, both auxin biosynthesis and transport contribute to the establishment and maintenance of maxima, minima, and auxin gradients, which are required for auxin-mediated growth and patterning processes in plants.[2,3,5,7]

For auxin signaling, the TRANSPORT INHIBITOR RESPONSE1 (TIR1)/AUXIN SIGNALING F-BOXs (AFBs)-AUXIN/INDOLE-3-ACETIC ACID (Aux/IAA) coreceptor-based transcriptional pathway has been well established by genetic and biochemical studies: IAA recruits transcriptional repressors Aux/IAA proteins to the TIR1/AFB F-box E3 ligases, which lead to their ubiquitination for subsequent degradation via the 26S proteasome, thus releasing downstream AUXIN RESPONSE FACTOR (ARF) transcription factors to regulate the expression of thousands of genes.[5,20,21] Our current understanding of the TIR1/AFB-Aux/IAA-mediated auxin pathway has also been improved by state-of-the-art live imaging and structural biological research.[22–24] Notably, TIR1/AFB auxin receptors, in addition to their roles as E3 ligases, were recently reported to also have an AMP cyclase activity needed for downstream transcriptional regulation.[25] Recent studies have also revealed that the PM-resident AUXIN BINDING PROTEIN1 (ABP1)/ABP1-LIKE PROTEINS (ABLs) and TRANSMEMBRANE KINASEs (TMKs) play crucial roles in auxin-induced apoplastic pH regulation, ROP (for Rho-related GTPases from plants) GTPase activation, and downstream protein phosphorylation events,[24,26–30] and thus related rapid growth regulation. Moreover, unlike other TIR1/AFB members functioning at the nucleus, AFB1 resides at the cytoplasm and regulates the fast root growth inhibition, which might be involved in root gravitropism.[31–35]

[1]MOE Key Laboratory for Cellular Dynamics, Center for Advanced Interdisciplinary Science and Biomedicine of IHM, Division of Molecular & Cell Biophysics, Hefei National Science Center for Physical Sciences at the Microscale, School of Life Sciences, Division of Life Sciences and Medicine, University of Science and Technology of China, Hefei 230027, China
[2]These authors contributed equally
[3]Lead contact
*Correspondence: lx023@ustc.edu.cn (X.L.), sunlf17@ustc.edu.cn (L.S.), sttan@ustc.edu.cn (S.T.)
https://doi.org/10.1016/j.isci.2024.110363

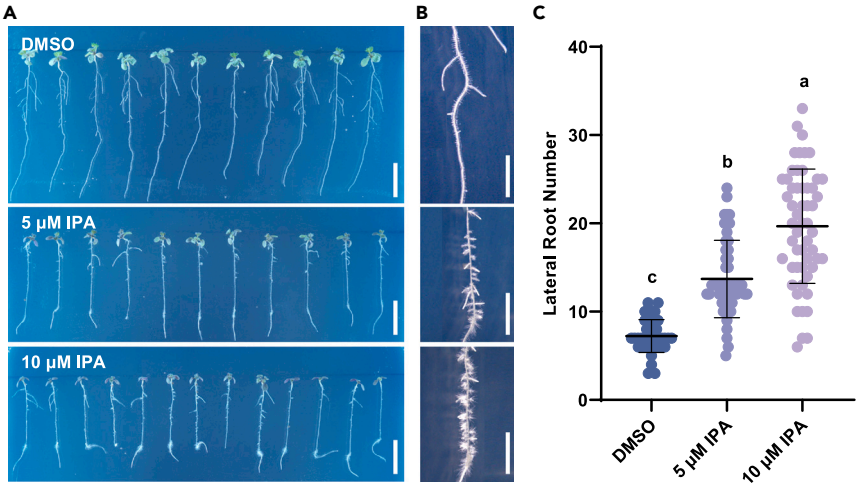

Figure 1. IPA exhibited auxinic activity in modulating root growth and development in *Arabidopsis*

(A and C) IPA treatment promoted LR formation. Representative images (A) and quantified lateral root numbers (C) of Col-0 plants. n = 40, 47, and 55, respectively. DMSO was used as the solvent control. Scale bars, 1 cm. Seven-day-old Col-0 plants were subsequently transferred to MS media supplemented with gradient concentrations of IPA for an additional 5 days. The emerged lateral roots were directly counted. Dots represent individual values, and lines indicate the mean ± SD. Different letters represent significant differences; $p < 0.05$; one-way ANOVA with Tukey's multiple comparison test.

(B) Representative images of lateral roots are shown. Scale bars, 5 mm. See also Figures S1–S4.

Indole-3-propionic acid (IPA) is a tryptophan metabolism-derived indole compound that is widely produced by various gut and soil microorganisms, including *Clostridium* and *Peptostreptococcus*.[36–38] Hormones or hormone-like compounds produced by rhizosphere soil microorganisms, such as IAA, are crucial for the growth and development of microorganisms and plants and for the coordination of microorganisms and plants.[3–5] Although IPA, a metabolite derived from gut microbes, has been widely studied for its ability to prevent and treat metabolic and neurological diseases in humans,[39,40] the effect of IPA on plants has not been fully elucidated. Previous studies reported that IPA inhibited root growth but seemingly independently of the TIR1 receptor.[41–44] Therefore, in this study, we explored the biological functions and underlying molecular mechanisms of IPA in plants and found that IPA regulates lateral root (LR) development via targeting the nuclear TIR1/AFB-Aux/IAA auxin signaling pathway.

RESULTS

IPA exhibited auxinic activity in modulating root growth and development in plants

To investigate the physiological effects of IPA, we explored the root phenotype of the model plant *Arabidopsis thaliana* grown on Murashige and Skoog (MS) plates supplemented with different concentrations of IPA. The results showed that 12-day-old *Arabidopsis* plants exhibited more LRs as well as more root hairs under constant treatment with IPA than the DMSO control (Figures S1A–S1D), resembling those observed under IAA treatment. Notably, when the concentration exceeded 10 μM, IPA strongly inhibited root growth and LR formation (Figures S1A–S1C). The plant hormone auxin regulates many growth and developmental processes, including root growth, lateral organ development, and root hair formation.[3,5,21,33] Auxin is known to promote LR formation and root hair growth. Next, to avoid the interference of inhibited root growth with LR formation, we transferred 7-day-old plants from normal MS plates to IPA for additional 5 days and found that IPA had a similar effect as IAA on promoting LR formation (Figures 1A–1C). Further physiological experiments with tobacco (*Nicotiana benthamiana*) revealed that similar phenotypes, i.e., inhibition of primary root elongation, promotion of LR formation, and root hair growth, were observed (Figures S2 and S3). To further confirm the effects of IPA on LR initiation, we treated LR primordia-probed reporters, including *PIN1::PIN1-GFP*[45] and *ARF19::NLS-GFP*[46] seedlings, with gradient concentrations of IPA and found that they formed more LR primordia under IPA treatment than the DMSO control (Figure S4A–S4F).

Taken together, these results indicate that IPA has an auxin-like activity in plants, including promotive effects on LR formation and root hair elongation. Additionally, IPA inhibited primary root elongation; however, this effect might not be mediated by the auxin signaling pathway, which will be described in the following, and this is consistent with the findings of previous reports.[41–44]

IPA activated the transcriptional auxin signaling pathway in *Arabidopsis*

Based on the aforementioned physiological effects of IPA, we speculated that IPA might be involved in the auxin pathway to regulate these physiological processes. To further explore the underlying molecular mechanisms, we assessed a series of auxin-responsive fluorescent reporters, including the *DR5v2-ntdTomato;DR5-n3GFP* dual reporter line,[47] which monitors the output of the TIR1/AFBs-Aux/IAAs-ARFs auxin signaling pathway. The DR5 signal significantly increased after IPA treatment, resembling the effect of IAA (Figures 2A and 2B), suggesting an

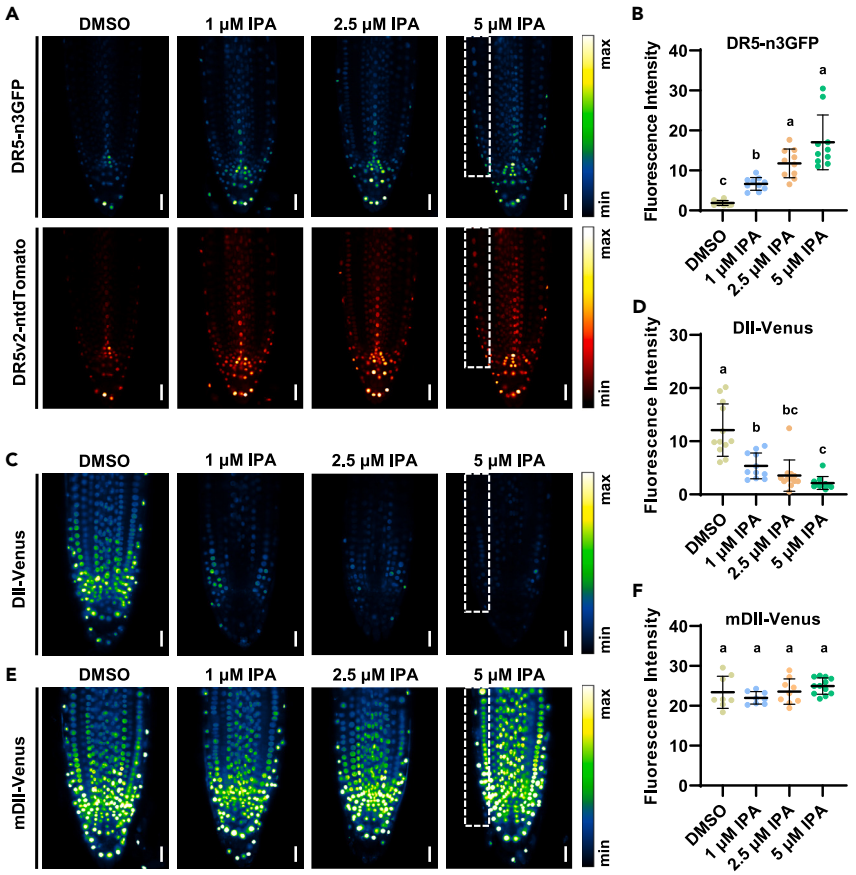

Figure 2. IPA activated the transcriptional auxin signaling pathway in *Arabidopsis*

(A and B) IPA application improved the auxin-responsive pattern of *DR5v2-ntdTomato;DR5-n3GFP*. Representative images (A) and quantified fluorescence intensity (B) of GFP on the root tip side. n = 10, 10, 10, 10. Four-day-old *DR5v2-ntdTomato;DR5-n3GFP* plants grown on normal MS plates were transferred to DMSO/IPA-containing plates for 24 h.

(C and D) DII-Venus responds rapidly to the auxin IPA. Representative images (C) and quantified fluorescence intensity (D) of Venus on the root tip side. n = 12, 11, 12, and 11, respectively. Four-day-old *DII-Venus* plants grown on normal plates were treated with DMSO/IPA-containing liquid for 30 min.

(E and F) mDII-Venus patients did not respond to IPA treatment. Representative images (E) and quantified fluorescence intensity (F) of Venus on the root tip side. n = 8, 8, 9, and 12, respectively. Four-day-old *mDII-Venus* seedlings grown on normal plates were treated with DMSO/IPA-containing liquid for 30 min. In (A), (C) and (E), root tips were imaged via confocal laser scanning microscopy (CLSM) for the GFP and tdTomato channels (A) and the Venus channel (C and E). 40×. Scale bars, 20 μm. In (B), (D), and (F), the dots represent individual values, and the lines indicate the means ± SDs. Different letters represent significant differences; $p < 0.05$; one-way ANOVA with Tukey's multiple comparison test. See also Figure S5.

activation of auxin signaling. Similar GFP-derived florescence activation was also observed for the tranditional *DR5rev::GFP* reporter[48] (Figures S5A and S5B), together suggesting that IPA activates the nuclear transcriptional auxin pathway.

We further used the *DII-Venus* reporter line,[49] which can reveal the rapid effect of the TIR1/AFB signaling pathway, to validate whether IPA functions via the canonical auxin pathway. DII-Venus is rapidly degraded following auxin perception via the TIR1/AFB pathway without the need for transcriptional activation.[49] The results showed that IPA treatment promoted the degradation of DII-Venus within 30 min, as rapidly as IAA did (Figures 2C–2F). Supported by these DR5- and DII-based observations, we hypothesize that IPA might activate endogenous auxin signaling through the nuclear TIR1/AFB-Aux/IAA-ARF pathway.

High concentrations of IPA showed strong inhibitory effects on root growth as well as interference with root gravitropism. We speculate that IPA treatment may also interfere with the transport or signaling of endogenous auxins. To further test this hypothesis, we used the *DR5v2-ntdTomato;DR5-n3GFP*[47] reporter (the GFP channel) to perform a root gravitropic response assay. The results showed that there was an increase in the DR5 signal at the lower side of the root tips in response to gravistimulation under 90° reorientation (Figure S5C). However, IPA treatment impaired this asymmetric DR5 redistribution (Figures S5C and S5D). Moreover, IPA inhibited the root bending under gravistimulation over time (Figures S5E and S5F). These results together suggest that IPA activates auxin signaling while also interfering with endogenous auxin signaling and/or transport, which might be due to the competition between IPA and endogenous IAA for auxin receptors or transporters.

IPA remodeled TIR1/AFBs-dependent transcriptome in *Arabidopsis*

To further investigate which pathway IPA might be involved in these effects, we carried out RNA sequencing (RNA-seq) profiling of 7-day-old *Arabidopsis* Col-0 and *tir1-1 afb2-3*[33] plants treated with IPA, IAA, or the solvent control DMSO, respectively. The results showed that IPA remodeled the global transcriptome in plants in a similar manner as IAA did, inducing the expression of numerous *Aux/IAAs*, *GH3s* (*GRETCHEN HAGEN3s*), *LBDs* (*LATERAL ORGAN BOUNDARIES DOMAINs*), *PINs*, *AUX1/LAXs*, and other auxin-responsive genes (Figures 3, S6, and S7). Notably, multiple genes involved in LR formation, such as *ARF19*, *LBD29*, *PUCHI*, *WOX11* (*WUSCHEL-RELATED HOMEOBOX11*), *PIN1*, *AUX1/LAXs*, and *GH3*, were also induced by IPA (Figures S6 and S7; Tables S1, S2, S3, and S4), consistently with the promotive effects of IPA on LR formation.

Venn diagrams revealed unique and shared sets of IPA-modulated DEGs (differentially expressed genes) and IAA-modulated DEGs between Col-0 and *tir1-1 afb2-3* (Figures 3C, 3D, and S7). Gene Ontology (GO) enrichment bubble diagrams and volcano plot diagrams showed that IPA treatment remodeled the expression of numerous genes in the auxin pathway (Figures 3A, 3B, and S6). Notably, IPA activated the expression of more genes than IAA did (Figures 3C, 3D, and S7A–S7D), suggesting potential distinct molecular mechanisms between IPA and IAA or possible dose effects. This difference might also account for the inhibitory effects of IPA on root growth, which seems not to be totally mediated by TIR1/AFBs-AUX/IAAs-ARFs, as reported previously.[41–44]

Furthermore, the Venn diagram contained more up-DEGs or down-DEGs in Col-0 than in *tir1-1 afb2-3* after IPA treatment (Figures 3C, 3D, and S7A–S7D), as did the heatmap (Figure S7E). This confirmed that *tir1-1 afb2-3* is less sensitive to IPA than is Col-0 in terms of the transcriptional auxin signaling pathway.

By performing quantitative reverse-transcription PCR (RT-qPCR) analysis, the relative expression levels of three known auxin-induced genes, namely, *GH3.3*, *GH3.5*,[50,51] and *LBD29*,[52] were confirmed to be upregulated by IPA in *Arabidopsis* seedlings (Figures 3E–3G). Detailed analysis with different concentrations of IPA revealed that the induction of these auxin-responsive genes by IPA was dose dependent, and the most effective concentrations of IPA and IAA are not the same for different genes (Figure S8). Taken together, these results demonstrated that IPA is involved in the nuclear TIR1/AFB-AUX/IAA-ARF auxin signaling, modulating plant LR formation.

IPA regulated LR development via the TIR1/AFB-Aux/IAA receptor complex

Next, we tested the IPA sensitivity of the TIR1/AFB-Aux/IAA-ARF-related mutants by growing the mutants in MS media supplemented with IPA (Figures S9–S21). In terms of the effects on LR induction, the auxin-insensitive *tir1-1*[53–55] mutants also exhibited markedly lower sensitivity to IPA than the Col-0 plants did (Figures S9A and S9B). Consistently, further microscopic analysis with the *DR5rev::GFP* auxin reporter revealed that the *tir1-1* mutation indeed decreased the sensitivity to IPA (Figures S10A and S10B), confirming the crucial roles of TIR1 in IPA perception. However, the primary root elongation of *tir1-1* was still sensitive to IPA (Figures S11A and S11B), suggesting that potentially different molecular mechanisms underlie the inhibition of primary root growth by IPA and IAA. Further physiological experiments with higher-order mutants revealed that the *tir1-1 afb2-3* and *tir1-1 afb2-1 afb3-1* mutants were also less sensitive to IPA than Col-0 in terms of LR formation (Figures 4 and S12) but not in primary root inhibition (Figure S13). The *arf7 arf19* mutant,[56] which is defective in auxin-controlled LR initiation, also exhibited similar insensitivity to LR induction to IPA (Figure S17). However, the primary root elongation of *arf7 arf19* was not inhibited by IPA (Figure S18). Interestingly, similar results were observed for the *afb5-5* and *afb4 afb5* mutants, which were less sensitive to IPA during LR induction (Figures S14–S16), suggesting the potential functional redundancy of *TIR1* and *AFBs* in IPA perception. Additionally, the *afb1-3* single mutant did not exhibit any changes in its sensitivity to IPA in these aforementioned tested phenotypes (Figures S19 and S20). Moreover, besides LRs, IPA also induced root hair growth in a TIR1/AFBs-dependent manner (Figure S21). Therefore, these results indicate that IPA regulates LR development and root hair growth via a set of TIR1/AFB receptors.

IPA directly targeted the TIR1/AFB-Aux/IAA receptor complex

Genetic and biochemical studies have well established the TIR1/AFB-AUX/IAA-ARF-mediated canonical auxin signaling pathway.[5,20,21] To address whether IPA interacts with TIR1/AFB coreceptors, a yeast two-hybrid assay was performed with TIR1 and IAA7 as a representative auxin coreceptor pair. Results showed that IPA promoted the interaction between TIR1 and IAA7 in yeast cells, though with a lower promotive effect than the same concentrations of IAA (Figure 5A). Next, we expressed and purified the TIR1 protein in complex with the ASK1 and IAA7 proteins and carried out a surface plasmon resonance (SPR) assay. Injection of the TIR1-ASK1 complex protein with either IPA or IAA indeed enhanced the interaction between TIR1 and IAA7, although IPA had a lower efficiency than IAA (Figure 5B), suggesting that IPA might bind to the TIR1-IAA7 coreceptors. Together with the cell biological and RNA-seq results, our data indicate that IPA could directly target to the TIR1/AFB-AUX/IAA auxin coreceptors in plants.

Overall, these aforementioned data support that IPA directly binds to the TIR1/AFB-Aux/IAA receptor complex and modulates plant root growth and development through TIR1/AFBs-mediated auxin signaling. Additionally, based on this feature, high concentrations of IPA might also modulate the endogenous auxin distribution by interfering with signaling or the transport of endogenous IAAs.

DISCUSSION

IPA is a tryptophan metabolism-derived indole compound produced by gut and soil microbes.[36,37] Our work revealed that IPA exhibits an auxinic activity in *Arabidopsis* seedlings primarily by modulating LR growth and development (Figure 6). Genetic and biochemical data indicate that IPA targets the TIR1/AFB-Aux/IAA pathway and thus regulates downstream gene transcription (Figure 6). These lines of evidence

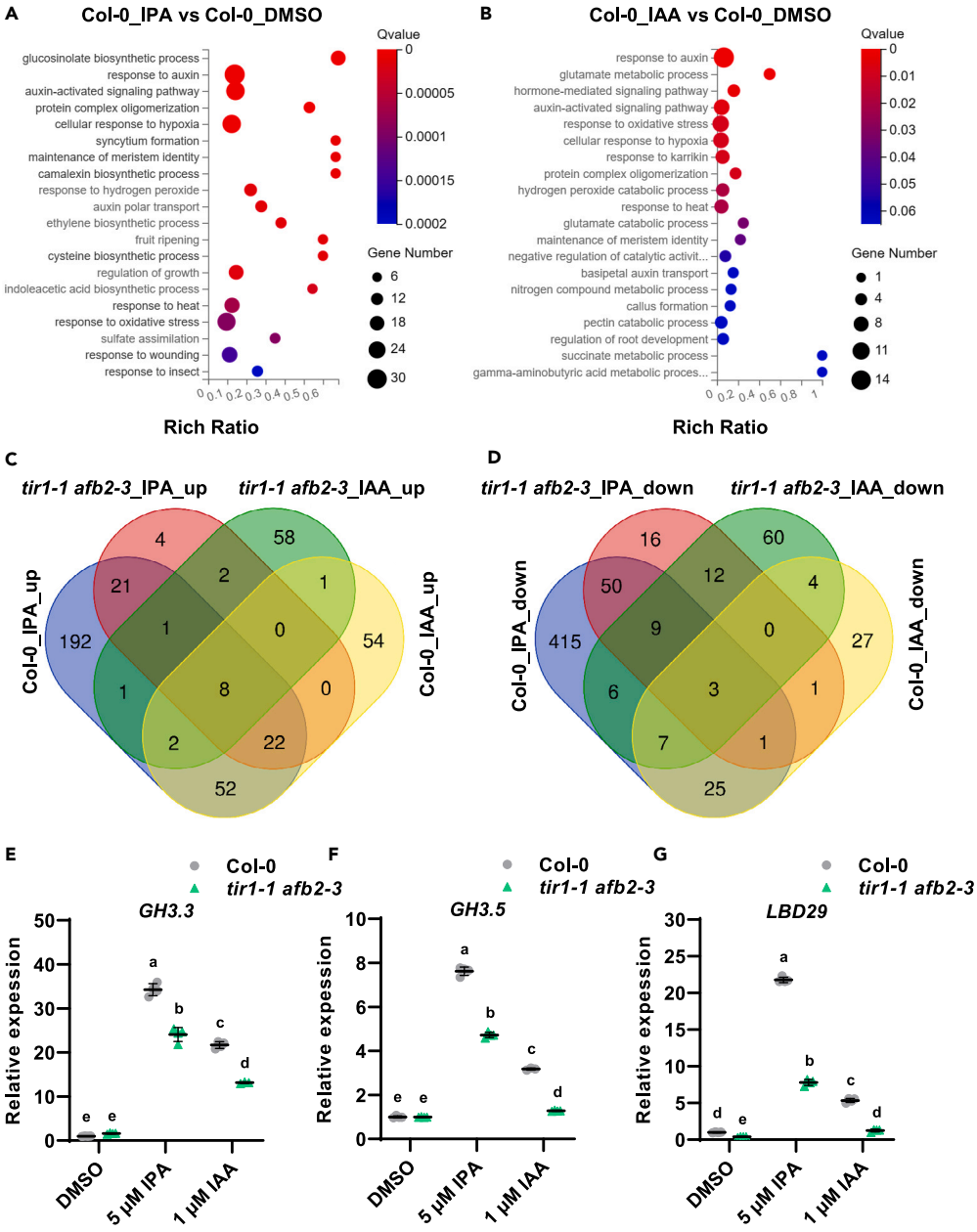

Figure 3. IPA treatment triggered global transcriptional changes, including auxin-responsive genes, in *Arabidopsis* seedlings

(A and B) GO enrichment analysis of a schematic representation of the RNA-seq data of 7-day-old Col-0 and *tir1-1 afb2-3* seedlings grown vertically on MS media and treated with 5 μM IPA, 1 μM IAA, or DMSO (as the mock control) for 3 h. Differentially expressed mRNAs in Col-0 seedlings treated with IPA (A) and IAA (B) versus those treated with DMSO. The X axis label represents the enrichment ratio, and the Y axis label represents the pathway. The size and color of the bubble represent the number of DEGs enriched in the pathway and enrichment significance, respectively.

(C and D) There were more upregulated DEGs or downregulated DEGs in Col-0 than in *tir1-1 afb2-3* after IPA treatment. Venn diagram of schematic representation of RNA sequencing data of 7-day-old Col-0 and *tir1-1 afb2-3* seedlings grown vertically on MS media and treated with 5 μM IPA, 1 μM IAA, or DMSO (as the mock control) for 3 h. Venn diagram showing the overlap of nondifferentially expressed genes (NDEGs) in the transcriptional data and DEGs. Each colored circle represents a different dataset, and areas of overlap indicate shared DEGs. (p value <0.05 and absolute log2 (fold change) > 0) in the translational data. (C) Venn diagram showing the overlap of upregulated NDEGs and DEGs in the transcriptional data of Col-0 or *tir1-1 afb2-3* after seedlings were treated with IPA for 3 h versus those treated with IAA. (D) Venn diagram showing the overlap of downregulated NDEGs and DEGs in the transcriptional data of Col-0 or *tir1-1 afb2-3* after seedlings were treated with IPA for 3 h versus those treated with IAA.

(E–G) RT-qPCR analysis showing the relative expression levels of three known auxin-induced genes (*GH3.3*, *GH3.5*, and *LBD29*) in seedlings. Col-0 (gray) or *tir1-1 afb2-3* (green) cells were mock infected or treated with DMSO, 5 μM IPA, or 1 μM IAA for 4 h. Dots represent individual values, and lines indicate the means ± SDs. $p < 0.05$; one-way ANOVA with Tukey's multiple comparison test. The normalized mean value of DMSO-treated WT cells was set at 1. See also Figures S6–S8, Tables S1, S2, S3, and S4.

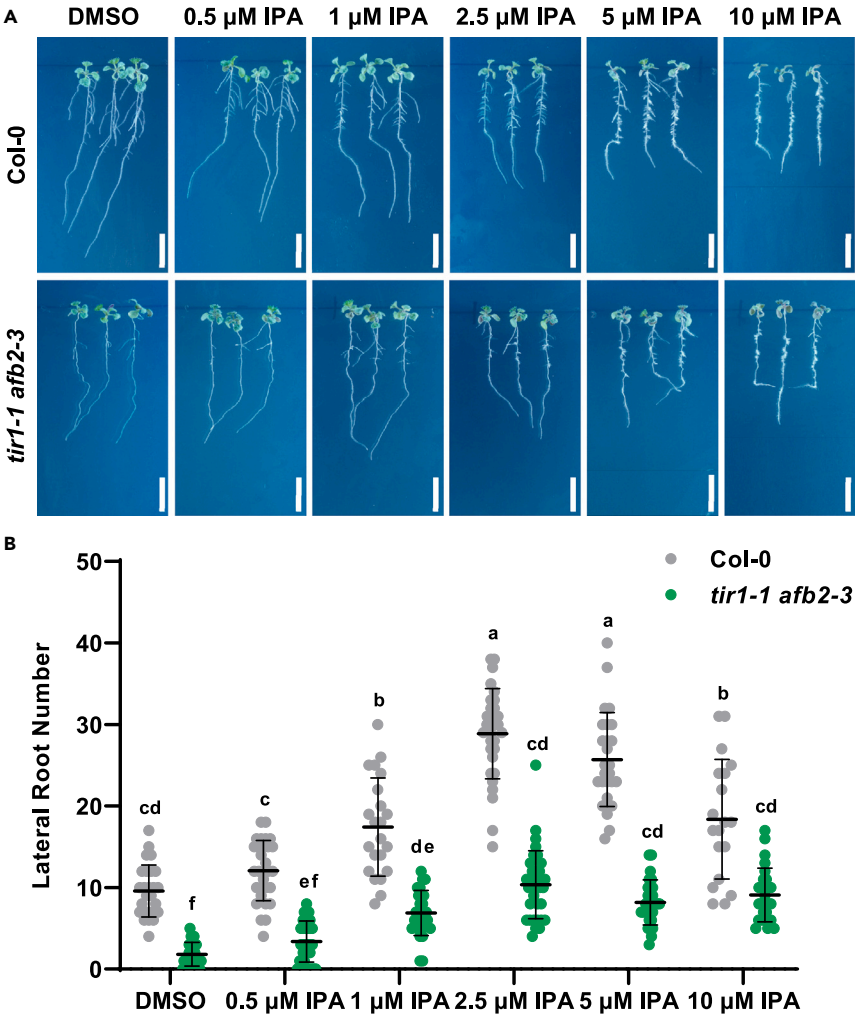

Figure 4. The induction of lateral root formation by IPA treatment was decreased in *tir1-1 afb2-3*

(A and B) *tir1-1 afb2-3* is less sensitive to IPA in terms of its ability to induce lateral root formation. Representative images (A) and quantified lateral root numbers (B) of *tir1-1 afb2-3*. Seven-day-old Col-0 or *tir1-1 afb2-3* were subsequently transferred to MS media supplemented with gradient concentrations of IPA for an additional 5 days. DMSO was used as the solvent control. The emerged lateral roots were directly counted. Scale bar, 1 cm n = 26, 30, 22, 31, 26, and 19 replicates for Col-0 seedlings and n = 32, 33, 27, 35, 27, and 26 replicates for *tir1-1 afb2-3* seedlings under the indicated treatments. Dots represent individual values, and lines indicate the mean ± SD. Different letters represent significant differences; $p < 0.05$; one-way ANOVA with Tukey's multiple comparison test. See also Figures S9–S21.

suggest that IPA may function as an interkingdom signaling molecule, coordinating the growth of different species, whose role in the natural ecosystem, however, requires further investigation. Although IAA participates in interspecies communication itself, our work potentially adds an additional layer to this signaling framework. Notably, although IPA and IAA have similar physiological effects on both primary root elongation and LR formation, the molecular mechanisms underlying primary root growth inhibition are likely distinct.[41–44] Further investigations might advance our understanding of the role of IPA in plant growth regulation.

In the soil, both IAA and IPA are synthesized by various rhizosphere microorganisms and are subsequently released into the environment.[36,37] The bioactivities of these compounds in plant cells involve interkingdom signaling between microbes and plants. Our work also suggested that microbe-derived IPA can modulate plant root growth and development. The molecular mechanism through which IPA targets the TIR1/AFB-Aux/IAA pathway also represents a potential genetic approach for future agricultural use.

Limitations of the study

While the current study has well established the molecular mechanisms of IPA targeting TIR1-IAA7 to regulate LR development and root hair growth, we cannot exclude that there could be other mechanisms underlying this process. Additionally, the interactions between microbes and plants are always complex in the nature, making it challenging to evaluate how much this IPA-TIR1-Aux/IAA pathway is involved.

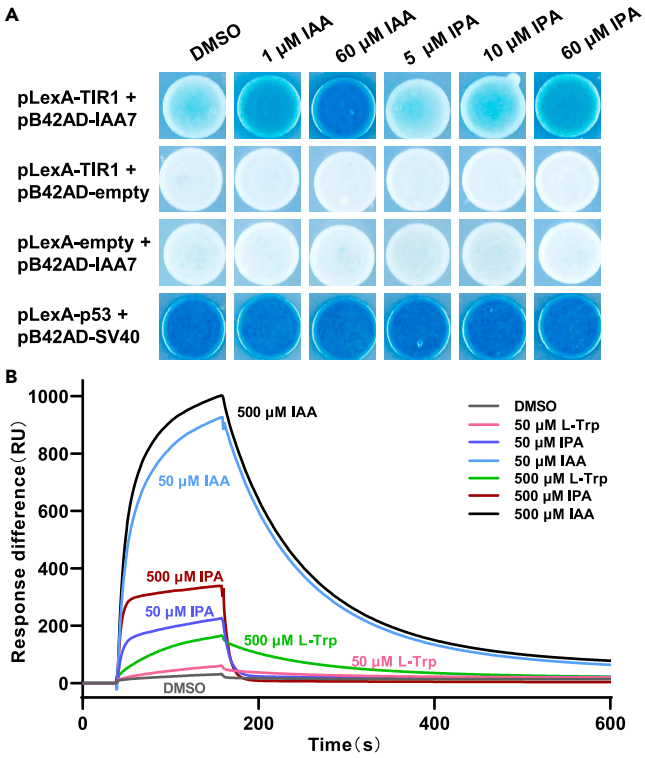

Figure 5. IPA-dependent TIR1–IAA7 interactions

(A) Yeast two-hybrid experiments revealed the promotive effect of IPA on the interaction between TIR1 with IAA7. Diploids containing LexA DBD-TIR1 and AD-IAA7 were generated and spotted in selective medium containing IAA or IPA. Activation of the expression of LacZ reporter gene evidenced IPA-induced TIR1 and IAA7 interactions 4 days after spotting. A control strain, containing the plasmids pB42AD-SV40 and pLexA-p53, was used as a positive control.

(B) SPR analysis of IPA and auxin-dependent TIR1-IAA7 interactions. The interactions and dissociations of compounds at different concentrations, including the DMSO control, 50 μM tryptophan, 50 μM IAA, 50 μM IPA, 500 μM tryptophan, 500 μM IAA, and 500 μM IPA, were tested between TIR1 and IAA7. The compounds were mixed with TIR1 in solution before injection. RU, resonance units.

STAR★METHODS

Detailed methods are provided in the online version of this paper and include the following:

- KEY RESOURCES TABLE
- RESOURCE AVAILABILITY
  - Lead contact
  - Materials availability
  - Data and code availability
- EXPERIMENTAL MODEL AND SUBJECT DETAILS
  - Plant materials and growth conditions
- METHOD DETAILS
  - Pharmacological treatments
  - Imaging by confocal laser scanning microscopy (CLSM)
  - Image analysis and morphological analysis
  - RNA-seq analysis
  - RT-qPCR analysis
  - Yeast two-hybrid (Y2H) assays
  - Protein expression and purification of IAA7
  - Protein expression and purification of TIR1
  - Surface plasmon resonance (SPR) analysis
  - Accession numbers
- QUANTIFICATION AND STATISTICAL ANALYSIS

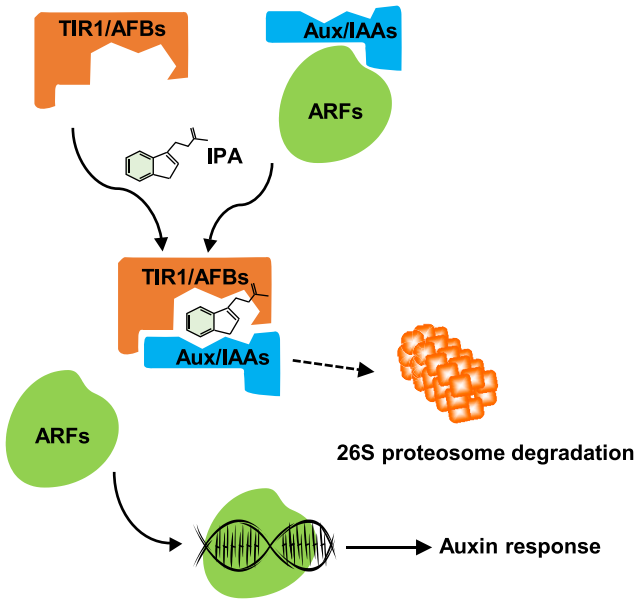

Figure 6. A hypothetical model for IPA and the auxin signaling pathway

Physiological effects of IPA on plants. TIR1/AFB receptors directly bind and sense IPA. In addition, IPA modulates plant growth and development through the canonical TIR1/AFB-Aux/IAA-ARF auxin signaling pathway.

SUPPLEMENTAL INFORMATION

Supplemental information can be found online at https://doi.org/10.1016/j.isci.2024.110363.

ACKNOWLEDGMENTS

We acknowledge Prof. Zhaojun Ding (Shandong University), Prof. Jing Zhang (China Agricultural University), Prof. Dolf Weijers (Wageningen University), and Prof. Mark Estelle (UCSD) for providing published *Arabidopsis* lines, and Prof. Jigang Li (China Agricultural University) for Y2H vectors and yeast strains. We thank Prof. Chengbin Xiang (USTC) and Prof. Zhong Zhao (USTC) for critical comments on the manuscript. This work was supported by the National Natural Science Foundation of China (32321001 to S.T. and L.S., 32322041 to L.S.), the Research Funds from the Center for Advanced Interdisciplinary Science and Biomedicine of IHM, Division of Life Sciences and Medicine, University of Science and Technology of China (QYPY20220012 to S.T., QYPY20230034 to L.S.), the Strategic Priority Research Program of the Chinese Academy of Sciences (XDB37020103 to L.S.), the Natural Science Foundation of Anhui Province (2008085MC90 to X.L., 2008085J15 to L.S.), the Double First-Class Initiative (YD9100002016 to S.T., YD9100002004 to L.S.), the start-up funding from the University of Science and Technology of China (GG9100007007, KY9100000026, KY9100000051, and KJ2070000079 to S.T.), and the Fundamental Research Funds for the Central Universities (WK9100000021 to S.T., WK9100000031 to L.S.).

AUTHOR CONTRIBUTIONS

X.L., L.S., and S.T. conceived and designed the research. Y.S. and C.Z. performed the physiological and cellular experiments and RNA-seq and analyzed the data under the supervision of S.T. Z.Y., J.X., and Y.L. performed the protein expression, purification, and SPR assays and analyzed the data under the supervision of X.L. and L.S. All the authors analyzed the data. Y.S., X.L., L.S., and S.T. wrote the manuscript with input from other coauthors, and all the authors revised it. All the authors contributed to the article and approved the submitted version.

DECLARATION OF INTERESTS

The authors declare no competing interests.

Received: April 17, 2024
Revised: May 30, 2024
Accepted: June 21, 2024
Published: June 24, 2024

REFERENCES

1. Vanneste, S., and Friml, J. (2009). Auxin: A trigger for change in plant development. Cell *136*, 1005–1016. https://doi.org/10.1016/j.cell.2009.03.001.
2. Tan, S., Luschnig, C., and Friml, J. (2021). Phoview of Auxin: Reversible Protein Phosphorylation in Auxin Biosynthesis, Transport and Signaling. Mol. Plant *14*, 151–165. https://doi.org/10.1016/j.molp.2020.11.004.
3. Friml, J. (2022). Fourteen stations of auxin. Cold Spring Harb. Perspect. Biol. *14*, a039859. https://doi.org/10.1101/cshperspect.a039859.
4. Yu, Z., Zhang, F., Friml, J., and Ding, Z. (2022). Auxin signaling: Research advances over the past 30 years. J. Integr. Plant Biol. *64*, 371–392. https://doi.org/10.1111/jipb.13225.
5. Carrillo-carrasco, V.P., Hernandez-garcia, J., Mutte, S.K., and Weijers, D. (2023). The birth of a giant : evolutionary insights into the origin of auxin responses in plants. EMBO J. *42*, e113018. https://doi.org/10.15252/embj.2022113018.
6. Zhao, Y. (2018). Essential roles of local auxin biosynthesis in plant development and in adaptation to environmental changes. Annu. Rev. Plant Biol. *69*, 417–435. https://doi.org/10.1146/annurev-arplant-042817-040226.
7. Brumos, J., Robles, L.M., Yun, J., Vu, T.C., Jackson, S., Alonso, J.M., and Stepanova, A.N. (2018). Local auxin biosynthesis is a key regulator of plant development. Dev. Cell *47*, 306–318.e5. https://doi.org/10.1016/j.devcel.2018.09.022.
8. Naseem, M., and Dandekar, T. (2012). The Role of Auxin-Cytokinin Antagonism in Plant-Pathogen Interactions. PLoS Pathog. *8*, 1003026. https://doi.org/10.1371/journal.ppat.1003026.
9. Yang, Z., Xia, J., Hong, J., Zhang, C., Wei, H., Ying, W., Sun, C., Sun, L., Mao, Y., Gao, Y., et al. (2022). Structural insights into auxin recognition and efflux by Arabidopsis PIN1. Nature *609*, 611–615. https://doi.org/10.1038/s41586-022-05143-9.
10. Su, N., Zhu, A., Tao, X., Ding, Z.J., Chang, S., Ye, F., Zhang, Y., Zhao, C., Chen, Q., Wang, J., et al. (2022). Structures and mechanisms of the Arabidopsis auxin transporter PIN3. Nature *609*, 616–621. https://doi.org/10.1038/s41586-022-05142-w.
11. Ung, K.L., Winkler, M., Schulz, L., Kolb, M., Janacek, D.P., Dedic, E., Stokes, D.L., Hammes, U.Z., and Pedersen, B.P. (2022). Structures and mechanism of the plant PIN-FORMED auxin transporter. Nature *609*, 605–610. https://doi.org/10.1038/s41586-022-05142-w.
12. Petrášek, J., Mravec, J., Bouchard, R., Blakeslee, J.J., Abas, M., Seifertová, D., Wiśniewska, J., Tadele, Z., Kubeš, M., Čovanová, M., et al. (2006). PIN proteins perform a rate-limiting function in cellular auxin efflux. Science *312*, 914–918. https://doi.org/10.1126/science.1123542.
13. Xia, J., Kong, M., Yang, Z., Sun, L., Peng, Y., Mao, Y., Wei, H., Ying, W., Gao, Y., Friml, J., et al. (2023). Chemical inhibition of Arabidopsis PIN-FORMED auxin transporters by the anti-inflammatory drug naproxen. Plant Commun. *4*, 100632. https://doi.org/10.1016/j.xplc.2023.100632.
14. Swarup, R., Friml, J., Marchant, A., Marchant, A., Ljung, K., Sandberg, G., Sandberg, G., Sandberg, G., Palme, K., Bennett, M., et al. (2001). Localization of the auxin permease AUX1 suggests two functionally distinct hormone transport pathways operate in the *Arabidopsis* root apex. Genes Dev. *15*, 2648–2653. https://doi.org/10.1101/gad.210501.2648.
15. Peret, B., Swarup, K., Ferguson, A., Seth, M., Yang, Y., Dhondt, S., James, N., Casimiro, I., Perry, P., Syed, A., et al. (2012). AUX/LAX Genes Encode a Family of Auxin Influx Transporters That Perform Distinct Functions during *Arabidopsis* Development. Plant Cell *24*, 2874–2885. https://doi.org/10.1105/tpc.112.097766.
16. Wu, G., Cameron, J.N., Ljung, K., and Spalding, E.P. (2010). A role for ABCB19-mediated polar auxin transport in seedling photomorphogenesis mediated by cryptochrome 1 and phytochrome B. Plant J. *62*, 179–191. https://doi.org/10.1111/j.1365-313X.2010.04137.x.
17. Henrichs, S., Wang, B., Fukao, Y., Zhu, J., Charrier, L., Bailly, A., Oehring, S.C., Linnert, M., Weiwad, M., Endler, A., et al. (2012). Regulation of ABCB1/PGP1-catalysed auxin transport by linker phosphorylation. EMBO J. *31*, 2965–2980. https://doi.org/10.1038/emboj.2012.120.
18. Titapiwatanakun, B., Blakeslee, J.J., Bandyopadhyay, A., Yang, H., Mravec, J., Sauer, M., Cheng, Y., Adamec, J., Nagashima, A., Geisler, M., et al. (2009). ABCB19/PGP19 stabilises PIN1 in membrane microdomains in *Arabidopsis*. Plant J. *57*, 27–44. https://doi.org/10.1111/j.1365-313X.2008.03668.x.
19. Ying, W., Wang, Y., Wei, H., Luo, Y., Ma, Q., Zhu, H., Janssens, H., Vukašinović, N., Kvasnica, M., Winne, J.M., et al. (2024). Structure and function of the Arabidopsis ABC transporter ABCB19 in brassinosteroid export. Science *383*, eadj4591. https://doi.org/10.1126/science.adj4591.
20. Calderon-villalobos, L.I., Tan, X., Zheng, N., and Estelle, M. (2010). Auxin Perception — Structural Insights. Cold Spring Harb. Perspect. Biol. *2*, a005546. https://doi.org/10.1101/cshperspect.a005546.
21. Mockaitis, K., and Estelle, M. (2008). Auxin receptors and plant development: A new signaling paradigm. Annu. Rev. Cell Dev. Biol. *24*, 55–80. https://doi.org/10.1146/annurev.cellbio.23.090506.123214.
22. Fendrych, M., Leung, J., and Friml, J. (2016). TIR1/AFB-Aux/IAA auxin perception mediates rapid cell wall acidification and growth of Arabidopsis hypocotyls. Elife *5*, e19048. https://doi.org/10.7554/eLife.19048.
23. Fendrych, M., Akhmanova, M., Merrin, J., Glanc, M., Hagihara, S., Takahashi, K., Uchida, N., Torii, K.U., and Friml, J. (2018). Rapid and reversible root growth inhibition by TIR1 auxin signalling. Nat. Plants *4*, 453–459. https://doi.org/10.1038/s41477-018-0190-1.
24. Li, L., Verstraeten, I., Roosjen, M., Takahashi, K., Rodriguez, L., Merrin, J., Chen, J., Shabala, L., Smet, W., Ren, H., et al. (2021). Cell surface and intracellular auxin signalling for H+ fluxes in root growth. Nature *599*, 273–277. https://doi.org/10.1038/s41586-021-04037-6.
25. Qi, L., Kwiatkowski, M., Chen, H., Hoermayer, L., Sinclair, S., Zou, M., del Genio, C.I., Kubeš, M.F., Napier, R., Jaworski, K., and Friml, J. (2022). Adenylate cyclase activity of TIR1/AFB auxin receptors in plants. Nature *611*, 133–138. https://doi.org/10.1038/s41586-021-04037-6.
26. Lin, W., Zhou, X., Tang, W., Takahashi, K., Pan, X., Dai, J., Ren, H., Zhu, X., Pan, S., Zheng, H., et al. (2021). TMK-based cell-surface auxin signalling activates cell-wall acidification. Nature *599*, 278–282. https://doi.org/10.1038/s41586-021-03976-4.
27. Franklin, K.A., Lee, S.H., Patel, D., Kumar, S.V., Spartz, A.K., Gu, C., Ye, S., Yu, P., Breen, G., Cohen, J.D., et al. (2011). PHYTOCHROME-INTERACTING FACTOR 4 (PIF4) regulates auxin biosynthesis at high temperature. Proc. Natl. Acad. Sci. *108*, 20231–20235. https://doi.org/10.1073/pnas.1110682108.
28. Kuhn, A., Roosjen, M., Koehorst, J., Dubey, S.M., Carrillo Carrasco, V.P., Kuhn, A., Roosjen, M., Boeren, S., Kohchi, T., Nishihama, R., and Monzer, A. (2024). RAF-like protein kinases mediate a deeply conserved , rapid auxin response. Cell *187*, 130–148.e17. https://doi.org/10.1016/j.cell.2023.11.021.
29. Yu, Y., Tang, W., Lin, W., Li, W., Zhou, X., Li, Y., Chen, R., Zheng, R., Qin, G., Cao, W., et al. (2023). ABLs and TMKs are co-receptors for extracellular auxin. Cell *186*, 5457–5471.e17. https://doi.org/10.1016/j.cell.2023.10.017.
30. Friml, J., Gallei, M., Gelová, Z., Johnson, A., Mazur, E., Monzer, A., Rodriguez, L., Roosjen, M., Verstraeten, I., Živanović, B.D., et al. (2022). ABP1-TMK auxin perception for global phosphorylation and auxin canalization. Nature *609*, 575–581. https://doi.org/10.1038/s41586-022-05187-x.
31. Serre, N.B.C., Wernerová, D., Vittal, P., Dubey, S.M., Medvecká, E., Jelínková, A., Petrášek, J., Grossmann, G., and Fendrych, M. (2023). The AUX1-AFB1-CNGC14 module establishes a longitudinal root surface pH profile. Elife *12*, e85193. https://doi.org/10.7554/eLife.85193.
32. Serre, N.B.C., Kralík, D., Yun, P., Slouka, Z., Shabala, S., and Fendrych, M. (2021). AFB1 controls rapid auxin signalling through membrane depolarization in *Arabidopsis thaliana* root. Nat. Plants *7*, 1229–1238. https://doi.org/10.1038/s41477-021-00969-z.
33. Prigge, M.J., Platre, M., Kadakia, N., Zhang, Y., Greenham, K., Szutu, W., Pandey, B.K., Bhosale, R.A., Bennett, M.J., Busch, W., and Estelle, M. (2020). Genetic analysis of the *Arabidopsis* TIR1/AFB auxin receptors reveals both overlapping and specialized functions. Elife *9*, e54740. https://doi.org/10.1101/529248.
34. Dubey, S.M., Han, S., Stutzman, N., Prigge, M.J., Medvecká, E., Platre, M.P., Busch, W., Fendrych, M., and Estelle, M. (2023). The AFB1 auxin receptor controls the cytoplasmic auxin response pathway in Arabidopsis thaliana. Mol. Plant *16*, 1120–1130. https://doi.org/10.1016/j.molp.2023.06.008.
35. Chen, H., Li, L., Zou, M., Qi, L., and Friml, J. (2023). Distinct functions of TIR1 and AFB1 receptors in auxin signaling. Mol. Plant *16*, 1117–1119. https://doi.org/10.1016/j.molp.2023.06.007.
36. Dodd, D., Spitzer, M.H., Van Treuren, W., Merrill, B.D., Hryckowian, A.J., Higginbottom, S.K., Le, A., Cowan, T.M., Nolan, G.P., Fischbach, M.A., and Sonnenburg, J.L. (2017). A gut bacterial pathway metabolizes aromatic amino acids into nine circulating metabolites. Nature *551*, 648–652. https://doi.org/10.1038/nature24661.
37. Ruth, E., Richards, L., and Schafer, P. (2021). Hormones as go-betweens in plant

microbiome assembly. Plant J. *105*, 518–541. https://doi.org/10.1111/tpj.15135.
38. Wlodarska, M., Luo, C., Kolde, R., d'Hennezel, E., Annand, J.W., Heim, C.E., Wlodarska, M., Luo, C., Kolde, R., Creasey, E.A., and Krastel, P. (2017). Indoleacrylic Acid Produced by Commensal Peptostreptococcus Species Suppresses Inflammation. Cell Host Microbe *22*, 25–37.e6. https://doi.org/10.1016/j.chom.2017.06.007.
39. Sehgal, R., de Mello, V.D., Männistö, V., Lindström, J., Tuomilehto, J., Pihlajamäki, J., and Uusitupa, M. (2022). Indolepropionic Acid, a Gut Bacteria-Produced Tryptophan Metabolite and the Risk of Type 2 Diabetes and Non-Alcoholic Fatty Liver Disease. Nutrients *14*, 4695. https://doi.org/10.3390/nu14214695.
40. Hwang, I.K., Yoo, K.-Y., Li, H., Park, O.K., Lee, C.H., Choi, J.H., Jeong, Y.-G., Lee, Y.L., Kim, Y.-M., Kwon, Y.-G., and Won, M.H. (2009). Indole-3-propionic acid attenuates neuronal damage and oxidative stress in the Ischemic Hippocampus. J. Neurosci. Res. *87*, 2126–2137. https://doi.org/10.1002/jnr.22030.
41. Uzunova, V.V., Quareshy, M., Del Genio, C.I., Napier, R.M., and Napier, R.M. (2016). Tomographic docking suggests the mechanism of auxin receptor TIR1 selectivity. Open Biol. *6*, 160139. https://doi.org/10.1098/rsob.160139.
42. Hoyerova, K., Hosek, P., Quareshy, M., Li, J., Klima, P., Kubes, M., Yemm, A.A., Neve, P., Tripathi, A., Bennett, M.J., and Napier, R.M. (2018). Auxin molecular field maps define AUX1 selectivity : many auxin herbicides are not substrates. New Phytol. *217*, 1625–1639. https://doi.org/10.1111/nph.14950.
43. Lee, S., Sundaram, S., Armitage, L., Evans, J.P., Hawkes, T., Kepinski, S., Ferro, N., and Napier, R.M. (2014). Defining Binding Efficiency and Specificity of Auxins for SCFTIR1/AFB- Aux/IAA Co-receptor Complex Formation. ACS Chem. Biol. *9*, 673–682. https://doi.org/10.1021/cb400618m.
44. Simon, S., Kubeš, M., Baster, P., Robert, S., Dobrev, P.I., Friml, J., Petrášek, J., and Zažímalová, E. (2013). Defining the selectivity of processes along the auxin response chain : a study using auxin analogues. New Phytol. *200*, 1034–1048. https://doi.org/10.1111/nph.12437.
45. Benková, E., Michniewicz, M., Sauer, M., Teichmann, T., Seifertová, D., Jürgens, G., and Friml, J. (2003). Local, efflux-dependent auxin gradients as a common module for plant organ formation. Cell *115*, 591–602. https://doi.org/10.1016/S0092-8674(03)00924-3.
46. Rademacher, E.H., Moller, B., Lokerse, A.S., Llavata-Peris, C.I., van den Berg, W., and Weijers, D. (2011). A cellular expression map of the Arabidopsis AUXIN RESPONSE FACTOR gene family. Plant J. *68*, 597–606. https://doi.org/10.1111/j.1365-313X.2011.04710.x.
47. Liao, C.-Y., Smet, W., Brunoud, G., Yoshida, S., Vernoux, T., and Weijers, D. (2015). Reporters for sensitive and quantitative measurement of auxin response. Nat. Methods *12*, 207–210. https://doi.org/10.1038/nmeth.3279.
48. Friml, J., Vieten, A., Sauer, M., Weijers, D., Schwarz, H., Hamann, T., Offringa, R., and Jürgens, G. (2003). Efflux-dependent auxin gradients establish the apical-basal axis of Arabidopsis. Nature *426*, 147–153. https://doi.org/10.1038/nature02085.
49. Brunoud, G., Wells, D.M., Oliva, M., Larrieu, A., Mirabet, V., Burrow, A.H., Beeckman, T., Kepinski, S., Traas, J., Bennett, M.J., and Vernoux, T. (2012). A novel sensor to map auxin response and distribution at high spatio-temporal resolution. Nature *482*, 103–106. https://doi.org/10.1038/nature10791.
50. Jagadeeswaran, G., Raina, S., Acharya, B.R., Maqbool, S.B., Mosher, S.L., Appel, H.M., Schultz, J.C., Klessig, D.F., and Raina, R. (2007). *Arabidopsis* GH3-LIKE DEFENSE GENE 1 is required for accumulation of salicylic acid, activation of defense responses and resistance to Pseudomonas syringae. Plant J. *51*, 234–246. https://doi.org/10.1111/j.1365-313X.2007.03130.x.
51. Zhang, Z., Li, Q., Li, Z., Staswick, P.E., Wang, M., Zhu, Y., and He, Z. (2007). Dual Regulation Role of GH3.5 in Salicylic Acid and Auxin Signaling during *Arabidopsis*-Pseudomonas syringae Interaction. Plant Physiol. *145*, 450–464. https://doi.org/10.1104/pp.107.106021.
52. Cho, H., Ryu, H., Rho, S., Hill, K., Smith, S., Audenaert, D., Park, J., Han, S., Beeckman, T., Bennett, M.J., et al. (2014). A secreted peptide acts on BIN2-mediated phosphorylation of ARFs to potentiate auxin response during lateral root development. Nat. Cell Biol. *16*, 66–76. https://doi.org/10.1038/ncb2893.
53. Dharmasiri, N., Dharmasiri, S., Weijers, D., Lechner, E., Yamada, M., Hobbie, L., Ehrismann, J.S., Jürgens, G., and Estelle, M. (2005). Plant development is regulated by a family of auxin receptor F box proteins. Dev. Cell *9*, 109–119. https://doi.org/10.1016/j.devcel.2005.05.014.
54. Kepinski, S., and Leyser, O. (2005). The *Arabidopsis* F-box protein TIR1 is an auxin receptor. Nature *435*, 446–451. https://doi.org/10.1038/nature03542.
55. Gray, W.M., Kepinski, S., Rouse, D., Leyser, O., and Estelle, M. (2001). Auxin regulates SCFTIR1-dependent degradation of AUX/IAA proteins. Nature *414*, 271–276. https://doi.org/10.1038/35104500.
56. Harper, R.M., Stowe-Evans, E.L., Luesse, D.R., Muto, H., Tatematsu, K., Watahiki, M.K., Yamamoto, K., and Liscum, E. (2000). The *NPH4* locus encodes the Auxin Response Factor ARF7, a conditional regulator of differential growth in aerial *Arabidopsis* tissue. Plant Cell *12*, 757–770. https://doi.org/10.1105/tpc.12.5.757.
57. Ruegger, M., Dewey, E., Gray, W.M., Hobbie, L., Turner, J., and Estelle, M. (1998). The *TIR1* protein of *Arabidopsis* functions in auxin response and is related to human *SKP2* and yeast *Grr1p*. Genes Dev. *12*, 198–207. https://doi.org/10.1016/s1369-5266(98)80055-1.
58. Cecchetti, V., Altamura, M.M., Brunetti, P., Petrocelli, V., Falasca, G., Ljung, K., Costantino, P., and Cardarelli, M. (2013). Auxin controls arabidopsis anther dehiscence by regulating endothecium lignification and jasmonic acid biosynthesis. Plant J. *74*, 411–422. https://doi.org/10.1111/tpj.12130.
59. Parry, G., Calderon-Villalobos, L.I., Prigge, M., Peret, B., Dharmasiri, S., Itoh, H., Lechner, E., Gray, W.M., Bennett, M., and Estelle, M. (2009). Complex regulation of the TIR1/AFB family of auxin receptors. Proc. Natl. Acad. Sci. USA *106*, 22540–22545. https://doi.org/10.1073/pnas.0911967106.
60. Okushima, Y., Fukaki, H., Onoda, M., Theologis, A., and Tasaka, M. (2007). ARF7 and ARF19 regulate lateral root formation via direct activation of LBD/ASL genes in Arabidopsis. Plant Cell *19*, 118–130. https://doi.org/10.1105/tpc.106.047761.
61. Estojak, J., Brent, R., and Golemis, E.A. (1995). Correlation of Two-Hybrid Affinity Data with In Vitro Measurements. Mol. Cell Biol. *15*, 5820–5829. https://doi.org/10.1128/mcb.15.10.5820.
62. Schneider, C.A., Rasband, W.S., and Eliceiri, K.W. (2012). NIH Image to ImageJ: 25 years of image analysis. Nat. Methods *9*, 671–675. https://doi.org/10.1038/nmeth.2089.
63. Schindelin, J., Arganda-Carreras, I., Frise, E., Kaynig, V., Longair, M., Pietzsch, T., Preibisch, S., Rueden, C., Saalfeld, S., Schmid, B., et al. (2012). Fiji: An open-source platform for biological-image analysis. Nat. Methods *9*, 676–682. https://doi.org/10.1038/nmeth.2019.
64. Savaldi-Goldstein, S., Baiga, T.J., Pojer, F., Dabi, T., Butterfield, C., Parry, G., Santner, A., Dharmasiri, N., Tao, Y., Estelle, M., et al. (2008). New auxin analogs with growth-promoting effects in intact plants reveal a chemical strategy to improve hormone delivery. Proc. Natl. Acad. Sci. USA *105*, 15190–15195. https://doi.org/10.1073/pnas.0806324105.

STAR★METHODS

KEY RESOURCES TABLE

REAGENT or RESOURCE	SOURCE	IDENTIFIER
Bacterial and virus strains		
Escherichia coli strain DH5α	Vazyme	Cat# C502-02
E. coli strain BL21 (DE3)	Vazyme	Cat# C504-02
E. coli strain DH10Bac	Invitrogen	Cat# 10361012
Chemicals, peptides, and recombinant proteins		
Murashige & Skoog Basal Medium including vitamins	Duchefa Biochemie	Cat# M0222.0050
Plant Agar	Duchefa Biochemie	Cat# P1001.1000
Indole 3-acetic acid (IAA)	Duchefa Biochemie	Cat# I0901.0025
3-Indolepropionic acid (IPA)	Sigma-Aldrich	Cat# 220027
Dimethyl sulfoxide (DMSO)	Sigma-Aldrich	Cat# D4540
L-Tryptophan	Sigma-Aldrich	Cat# T0254
Cellfectin II Reagent	Thermo Fisher Scientific	Cat# 10362100
Flag peptide	Sigma Aldrich	Cat# F3290
Flag-TIR1 recombinant protein	this paper	N/A
6×His-IAA7 recombinant protein	this paper	N/A
6×His-ASK1 recombinant protein	this paper	N/A
Yeast Nitrogen Base W/O Amino Acids	Coolaber	Cat# PM2070
YPDA Medium	Coolaber	Cat# PM2011
D-Glucose, anhydrous	biosharp	Cat# BS099
Do Summplement-His/-Trp/-Ura	Takara	Cat# 630424
D- (+)-Raffinose	Coolaber	Cat# CR9421
D- (+)-Galactose	Coolaber	Cat# CG5481
$Na_2HPO_4 \cdot 12H_2O$	SCR®	Cat# 10020318
$NaH_2PO_4 \cdot 2H_2O$	SCR®	Cat# 20040718
FastDigest EcoRI	NEB BioLabs	Cat# R0101S
ClonExpress II One Step Cloning Kit	Vazyme	Cat# C112-02
Critical commercial assays		
Trelief RNAprep FastPure Tissue & Cell Kit	Tsingke	Cat# TSP413
PrimeScript RT Master Mix (Perfect Real Time)	Takara	Cat# RR036A
2 × Q3 SYBR qPCR Master Mix (Universal)	Tolobio	Cat# 22204
Series S Sensor Chip CM5	Cytiva	Cat# 10343441
Ni-NTA agarose	Qiagen	Cat# 30250
anti-Flag M2 affinity gel	Sigma-Aldrich	Cat# A2220
Superdex 200 Increase 10/300 GL column	Cytiva	Cat# 28990944
Deposited data		
RNAseq data	this paper	SRA: PRJNA1117596
Experimental models: Cell lines		
Sf-9 insect cell	Gibco	Cat# 11496015
Experimental models: Organisms/strains		
Arabidopsis thaliana: wild-type (Col-0)	N/A	N/A
A. thaliana: *tir1-1*	Ruegger et al.[57]	N/A

(*Continued on next page*)

Continued

REAGENT or RESOURCE	SOURCE	IDENTIFIER
A. thaliana: *afb1-3*	Cecchetti et al.[33,58]	N/A
A. thaliana: *tir1-1 afb2-3*	Ruegger et al.[57]	N/A
A. thaliana: *tir1-1 afb2-1 afb3-1*	Cecchetti et al.[33,58]	N/A
A. thaliana: *afb5-5*	Prigge et al.[33,59]	N/A
A. thaliana: *afb4 afb5*	Prigge et al.[33,59]	N/A
A. thaliana: *arf7 arf19*	Okushima et al.[60]	N/A
A. thaliana: *DR5rev::GFP*	Friml et al.[48]	N/A
A. thaliana: *DR5v2-tdTomato; DR5-n3GFP*	Liao et al.[47]	N/A
A. thaliana: *DII-Venus*	Brunoud et al.[49]	N/A
A. thaliana: *mDII-Venus*	Brunoud et al.[49]	N/A
A. thaliana: *PIN1::PIN1-GFP*	Benková et al.[45]	N/A
A. thaliana: *ARF19::NLS-GFP* (*pARF19-n3GFP*)	Rademacher et al.[46]	N/A
EGY48	Estojak et al.[61]	
Oligonucleotides		
Primer for RT-qPCR: GH3.3 Forward Primer: CATCACAGAGTTCCTCACAAGC	this paper	N/A
Primer for RT-qPCR: GH3.3 Reverse primer: GTCGGTCCATGTCTTCATCA	this paper	N/A
Primer for RT-qPCR: GH3.5 Forward Primer: CATCTCTGAGTTCCTCACAAGC	this paper	N/A
Primer for RT-qPCR: GH3.5 Reverse primer: CCTCTTCGATTGTTGGCATT	this paper	N/A
Primer for RT-qPCR: IAA5 Forward primer: TGAAGGAAAGTGAATGTGTACCAA	this paper	N/A
Primer for RT-qPCR: IAA5 Reverse primer: GCACGATCCAAGGAACATTT	this paper	N/A
Primer for RT-qPCR: IAA19 Forward primer: TGGTGACAACTGCGAATACGTTAC	this paper	N/A
Primer for RT-qPCR: IAA19 Reverse primer: CGTCTACTCCTCTAGGCTGCAG	this paper	N/A
Primer for RT-qPCR: LBD29 Forward primer: GCTAGGCTTCAAGATCCCATC	this paper	N/A
Primer for RT-qPCR: LBD29 Reverse primer: TGTGCTGCTTGTTGCTTTAGA	this paper	N/A
Primer for RT-qPCR: ACTIN7 Forward primer: CCGGTATTGTGCTCGATTCTG	this paper	N/A
Primer for RT-qPCR: ACTIN7 Reverse primer: TTCCCGTTCTGCGGTAGTGG	this paper	N/A
Primer for homologous recombination of pLexA and TIR1-Forward primer: AACGGCGACTGGC TGATGCAGAAGCGAATAGCC	this paper	N/A
Primer for homologous recombination of pLexA and TIR1-Reverse primer: GCTTGGCTGCAGGTCGATTAT AATCCGTTAGTAGTAATGATTTGCC	this paper	N/A
Primer for homologous recombination of pB42AD and IAA7-Forward primer: GATTATGCCTCTCCC ATGATCGGCCAACTTATGAACC	this paper	N/A

(*Continued on next page*)

Continued

REAGENT or RESOURCE	SOURCE	IDENTIFIER
Primer for homologous recombination of pB42AD and IAA7-Reverse primer: AGAAGTCCAAAGCTTTCAAGA TCTGTTCTTGCAGTACTTCTCCAT	this paper	N/A
Primer for homologous recombination of pLexA and p53-Forward primer: AACGGCGACTG GCTGATGCCTGTCACCGAGACCC	this paper	N/A
Primer for homologous recombination of pLexA and p53-Reverse primer: TTGGCTGCAGGTC GATCAGTCTGAGTCAGGCCCCA	this paper	N/A
Primer for homologous recombination of pB42AD and SV40-Forward primer: GATTATGCCTC TCCCATGGGAACTGATGAATGGGAGC	this paper	N/A
Primer for homologous recombination of pB42AD and SV40-Reverse primer: AGAAGTCCAAA GCTTTATGTTTCAGGTTCAGGGGGAG	this paper	N/A
Primer for pFastBac-Flag-TIR1, Forward primer: GATGACGATGACAAGCATATGCA GAAGCGAATAGCCTTG	this paper	N/A
Primer for pFastBac-Flag-TIR1, Reverse primer: GTACCGC ATGCCTCGACCTCGAGTTATAATCCGTTAGTAG	this paper	N/A
Primer for pET-15d-6×His-IAA7, Forward primer: GAAGTTGATGCACATATGATCGGCCAACTTATG	this paper	N/A
Primer for pET-15d-6×His-IAA7, Reverse primer: AGCAGCCGGATCCTCGAGTCAAGATCTGTTCTTGCAG	this paper	N/A
Primer for pFastBac-6×His-ASK1, Forward primer: GATGCTGGCAGCGGCCAT ATGTCTGCGAAGAAGATTGTG	this paper	N/A
Primer for pFastBac-6×His-ASK1, Reverse primer: GTACCGCATGCCTCGACCTC GAGTCATTCAAAAGCCCATTG	this paper	N/A
Recombinant DNA		
Plasmid pFastBac-Flag-TIR1	this paper	N/A
Plasmid pET-15d-6×His-IAA7	this paper	N/A
Plasmid pFastBac-6×His-ASK1	this paper	N/A
Plasmid pLexA-TIR1	this paper	N/A
Plasmid pB42AD-IAA7	this paper	N/A
Plasmid pLexA-p53	this paper	N/A
Plasmid pLexA-SV40	this paper	N/A
Plasmid p8op-lacZ	Estojak et al.[61]	N/A
pFastBac1	Invitrogen	Cat# 10359-016
pET15D	Novagen	N/A
Software and algorithms		
ImageJ	Schneider et al.[62]	https://imagej.nih.gov/ij/
Fiji	Schindelin et al.[63]	https://fiji.sc/
ZEN	ZEISS	https://www.zeiss.com.cn/
GraphPad Prism 8.3.0 (538)	Graphpad Software, USA	https://www.graphpad.com/scientific-software/prism/
Biacore T200 Evaluation Software Version 3.0	Cytiva	N/A
Origin 2023	OriginLab	https://www.originlab.com/

RESOURCE AVAILABILITY

Lead contact

Further information and requests for resources and reagents should be directed to and will be fulfilled by the Lead Contact, (sttan@ustc.edu.cn).

Materials availability

This study did not generate new unique reagents and the materials generated in this study are available from the corresponding author.

Data and code availability

- RNA-seq data have been deposited at NCBI and are publicly available as of the date of publication. Accession numbers are listed in the key resources table.
- This study did not report any original code.
- Any additional information required to reanalyze the data reported in this paper is available from the lead contact upon request.

EXPERIMENTAL MODEL AND SUBJECT DETAILS

Plant materials and growth conditions

The *Arabidopsis thaliana* (L.) mutants and transgenic plants were all in the Columbia-0 (Col-0) ecotype background. The marker lines *DII-Venus*,[49] *mDII-Venus*,[49] *DR5v2-ntdTomato;DR5-n3GFP*[47], *DR5rev::GFP*,[48] *PIN1::PIN1-GFP*,[45] and *ARF19::NLS-GFP (pARF19-n3GFP)*[46] were reported previously. The *tir1-1*,[57] *arf7 arf19*,[60] *tir1-1 afb2-3*,[57,64] *tir1-1 afb2-1 afb3-1*,[58] *afb1-3*,[58] *afb5-5*,[33,59] and *afb4 afb5*[33,59] mutants in the Col-0 background were also reported previously, and Col-0 was used as a control.

For phenotyping of seedlings or pharmacological experiments, surface-sterilized seeds were sown on solid Murashige and Skoog (MS) media [0.5× MS media supplemented with 1% (w/v) sucrose and 0.8% (w/v) phytoagar; MES buffer, pH 5.9]; stratified at 4°C for 2 days; and subsequently grown vertically in a growth chamber at 21°C with a 16-h light/8-h dark photoperiod. For microscopic analysis, four-day-old plants from different reporter lines were transferred to MS media supplemented with gradient concentrations of IPA for 24 or 48 h as indicated.

METHOD DETAILS

Pharmacological treatments

For long-term growth assays, *Arabidopsis* seeds were sown on vertical plates with MS media supplemented with the indicated chemicals, including 3-indolepropionic acid (Sigma, 220027) and dimethyl sulfoxide (DMSO; Sigma, D4540) as the mock control. After 2 d of stratification, the plants were transferred to a growth chamber as described in the "Plant material and growth conditions" session, the length of the roots was measured, and the phenotype of the roots was observed after an additional 7 or 12 days of growth. For lateral root induction assays, 7-d-old plants were grown on MS media and subsequently transferred to 0.5×MS media supplemented with various concentrations of the test compounds as described in the figure legends. After 5 days, the number of lateral roots was counted. For the observation of DR5v2-ntdTomato;DR5-n3GFP and DR5rev::GFP, 4-d-old plants were subsequently transferred to 0.5×MS solid media supplemented with gradient concentrations of IPA, after which GFP and ntdTomato fluorescence at the root tip regions was observed. For DII-Venus and mDII-Venus observation, 4-d-old plants were subsequently transferred to 0.5×MS liquid media supplemented with gradient concentrations of IPA or DMSO, after which the Venus fluorescence at the root tip regions was observed. For PIN1::PIN1-GFP and ARF19::NLS-GFP observation, 6-d-old plants were transferred to 0.5×MS solid media supplemented with gradient concentrations of IPA, after which GFP fluorescence at the primordium regions was observed.

Imaging by confocal laser scanning microscopy (CLSM)

Fluorescence imaging of the reporter lines was performed using a Zeiss LSM980 confocal laser scanning microscope with a GaAsP detector (Zeiss, Germany). The default settings (smart mode) were used for imaging proteins tagged with GFP (excitation, 488 nm; emission, 495–545 nm), tdTomato (excitation, 561 nm; emission, 571–630 nm), or Venus (excitation, 514 nm; emission, 524–580 nm). All of the images were obtained at 8-bit depth with 2× line averaging.

Image analysis and morphological analysis

For observation of the seedling root phenotype, photographs were taken using a camera (Sony A6000 with a macro lens), and the primary root length or root tip angles were subsequently analyzed with the ImageJ software. The lateral root numbers were counted directly. The root hairs were observed using the NIS-Elements program with a stereomicroscope (Nikon SMZ18). For observation of fluorescence in the roots, all the images were obtained using a laser-scanning confocal microscope (Zeiss LSM980) as described above, and the fluorescence intensity was measured using ImageJ.

RNA-seq analysis

For RNA-seq analysis, 7-d-old *Arabidopsis* plants were treated with 1 μM IAA, 5 μM IPA or DMSO for 3 h. Each RNA sample was prepared from a pool of Col-0 or *tir1-1 afb2-3* plants (200 mg) treated with the tested compounds. Three independent RNA samples for each condition were used for the following analyses, and 1 μg of each RNA sample was used for library preparation. RNA extraction, library preparation and RNA-seq were performed by BGI using an BGISEQ platform resulting in approximately 44 million reads per sample. Raw RNA-seq reads were subjected to quality checking and trimming to remove adaptor sequences, contamination and low-quality reads. The trimmed reads of each sample were aligned to the publicly available reference genome of Arabidopsis (TAIR10, https://support.illumina.com/sequencing/sequencing_software/igenome.html) using HISAT2 version 2.0.4 on default parameters. Data analyses were performed with the Dr.Tom platform of BGI.

RT-qPCR analysis

Reverse transcription-quantitative PCR (RT-qPCR) was used to examine the transcript levels of *GH3.3, GH3.5, IAA5, IAA19* and *LBD29* in Col-0 plants treated with 1 μM IAA, 5 μM IPA or DMSO, respectively; *ACTIN7* (*AT5G09810*) was used as an internal reference. In detail, total RNA was extracted from the indicated tissues using Trelief RNAprep FastPure Tissue & Cell Kit (Tsingke, TSP413), and DNase was added to digest the genomic DNA. Then, 1 μg of the RNA sample was reversely transcribed (Takara, RR036A). The resulting cDNA of the corresponding genes and *ACTIN7* was analyzed using SYBR qPCR Master Mix (Tolobio, 22204) with a Bio-Rad CFX Connect Real-Time System. The relative transcript level of the examined genes was normalized to the expression of *ACTIN7* and was calculated by setting the WT or a certain tissue as 1, and the data are presented as the mean ± SD. from three biological replicates.

Yeast two-hybrid (Y2H) assays

By homologous recombination, *TIR1* and *IAA7* coding sequences were cloned into the Y2H bait vector pLexA and to the prey vector pB42AD, respectively, after amplifying using the following primer pairs: *TIR1*, AACGGCGACTGGCTGATGCAGAAGCGAATAGCC and GCTTGGCTG CAGGTCGATTATAATCCGTTAGTAGTAATGATTTGCC; *IAA7*, GATTATGCCTCTCCCATGATCGGCCAACTTATGAACC and AGAAGTCC AAAGCTTTCAAGATCTGTTCTTGCAGTACTTCTCCAT. Bait and pray constructs were co-transformed into *Saccharomyces cerevisiae* strain EGY48 containing a p8opLacZ vector and transformants were selected on SD plates supplemented with –Ura/–His/–Trp dropout solution.[61] To test the interaction between TIR1 and IAA7 proteins, transformed yeast colonies were plated on SD-galactose/raffinose inducing medium containing –Ura/–His/–Trp dropout supplement, 80 μg/mL X-Gal, and various concentrations of compounds, indicated in corresponding figures. Plates were incubated for 3–4 days at 30°C. A control strain, containing the plasmids pB42AD-SV40 and pLexA-p53, was used as a positive control.

Protein expression and purification of IAA7

The full-length *Arabidopsis thaliana* IAA7 was cloned and inserted into the pET-15d vector (Invitrogen) with six histidine residues in the N-terminus. The plasmid was introduced into BL21 (DE3) competent cells (Invitrogen). IAA7 expression was induced by adding 0.2 mM IPTG and culturing at 37°C for 4 h. The bacteria were collected by centrifugation, and the pellet was suspended in lysis buffer containing 25 mM Tris-HCl (pH 8.0), 150 mM NaCl, and 1 mM phenylmethylsulfonyl fluoride (PMSF) and disrupted by sonication. The cell extract was centrifuged at 42,000 × g for 1 h, and the supernatant was loaded onto Ni-NTA resin (Qiagen). The resin was washed three times with buffer containing 25 mM Tris-HCl (pH 8.0), 150 mM NaCl and 25 mM imidazole. Then, the protein was eluted with 25 mM Tris-HCl (pH 8.0) and 250 mM imidazole. IAA7 was further purified by a Source 15S cation exchange column (Cytiva). The peak fractions were collected for SPR assays.

Protein expression and purification of TIR1

The full-length CDS of *Arabidopsis thaliana TIR1* was cloned and inserted into the pFastBac vector (Invitrogen) with a flag tag at the N-terminus. The full-length CDS of *Arabidopsis thaliana ASK1* was cloned and inserted into the pFastBac vector with a six-histidine tag in the N-terminus. The recombinant virus was generated by Sf9 insect cells (Invitrogen). Sf9 cells were transfected with P2 virus containing TIR1 and ASK1 at a ratio of 1:1. The cells were collected by centrifugation, and the pellet was resuspended in lysis buffer containing 25 mM Tris-HCl (pH 7.4), 150 mM NaCl, and 1 mM PMSF. The cells were disrupted by sonication, and the cell extract was centrifuged at 42,000 × g for 1 h. The supernatant was incubated with anti-FLAG M2 affinity gel (Sigma Aldrich) at 4°C for 30 min. The resin was washed three times with buffer containing 25 mM Tris-HCl (pH 7.4) and 150 mM NaCl. The protein was eluted with 25 mM Tris-HCl (pH 7.4), 150 mM NaCl and 200 μg/mL Flag peptide. The TIR1-ASK1 protein was further purified with a Superdex 200 Increase column (Cytiva). The peak fractions were collected for SPR assays.

Surface plasmon resonance (SPR) analysis

SPR measurements were performed using Biacore T200 systems (Biacore GE Healthcare Biosciences). IAA7 protein was immobilized onto a Series S CM5 sensor chip (Cytiva) with 9,454 resonance units (RU). The purified TIR1-ASK1 proteins were administered at a concentration of 20 μg/mL, and various concentrations of IAA (Duchefa Biochemie), IPA (Sigma Aldrich), or tryptophan (Sigma Aldrich) were injected over the chip at a flow rate of 30 μL/min in HBS-EP buffer containing 20 mM HEPES (pH 7.4), 150 mM NaCl, 3 mM EDTA, 0.05% (w/v) P20 and 5% DMSO. The data were analyzed with Biacore T200 Evaluation Software Version 3.0 (Biacore GE Healthcare Biosciences).

Accession numbers

Published sequence data from this article can be found in the Arabidopsis Genome Initiative or enBank/EMBL databases. The accession numbers used are as follows: *NPH4/ARF7* (AT5G20730), *ARF19* (AT1G19220), *AXR2/IAA7* (AT3G23050), *TIR1* (AT3G62980), *AFB1* (AT4G03190), *AFB2* (AT3G26810), *AFB3* (AT1G12820), *AFB4* (AT4G24390), and *AFB5* (AT5G49980).

QUANTIFICATION AND STATISTICAL ANALYSIS

Most of the experiments were repeated at least three times independently, each yielding similar results. For measurements of primary root length and root tip angles, photographs or scans were analyzed with the ImageJ program (https://imagej.nih.gov/ij/download.html)[62] or Fiji (https://fiji.sc/).[63] The fluorescence intensity of the CLSM images was quantified by Fiji (https://fiji.sc/).[63] Data visualization and statistical analysis were mostly performed with GraphPad Prism 8. For the bending curvatures of the root tips, polar graphs were generated with Origin 2023. *n* and *p* values are indicated in the figures and legends, respectively.